An Equation-of-State Contribution for Polar Components: Quadrupolar Molecules

Joachim Gross
Conceptual Process Engineering, BASF AG, GIC/P–Q920, 67056 Ludwigshafen, Germany

DOI 10.1002/aic.10502
Published online June 13, 2005 in Wiley InterScience (www.interscience.wiley.com).

An equation-of-state (EOS) contribution for quadrupolar interactions is developed based on a third-order perturbation theory. Model constants are adjusted to comprehensive molecular simulation data for vapor–liquid equilibria of the two-center Lennard–Jones (2CLJ) plus pointquadrupole fluid from the literature. Molecular elongations L from 0 (spherical) to 0.8 are covered by the simulation data. The EOS is suited for both, the 2CLJ fluid and the tangent-sphere Lennard–Jones framework. It is applied to pure components and mixtures of real substances with the perturbed-chain statistical associating fluid theory (PC-SAFT) EOS. It is possible to use tabulated values of quadrupolar moments (independently determined) directly in the EOS, so that no additional pure component parameter is introduced. Compared with the case where quadrupolar interactions are not specifically accounted for, the proposed model gives a systematic improvement of pure component properties and of mixture phase equilibria of strong quadrupolar components, such as carbon dioxide, and the absolute value of the required binary interaction parameter is significantly reduced.* © 2005 American Institute of Chemical Engineers *AIChE J,* 51: 2556–2568, 2005
Keywords: equation of state, polar, perturbation theory, mixtures, nonspherical molecules, SAFT

Introduction

The effect of a molecule's permanent electrostatic moments on the macroscopic physical behavior of the involved system has long since attracted research interest and it is well accepted that equations of state (EOS) attain a more predictive character when the quadrupolar interactions are individually considered. The strong permanent quadrupolar moment of carbon dioxide, for example, causes relatively high solubilities of polar compounds in carbon dioxide, enabling its use as a solvent in many novel chemical processes as well as in food and in pharmaceutical industries.[1] On a molecular level, the permanent quadrupolar charge distribution, where negative partial charges exist on both molecular ends and a double-positive partial charge is located in the center, results in specific molecular interactions.

Perturbation theories are often applied to describe polar interactions. Gubbins and Twu[2] developed a set of readily applicable expressions to account for dipolar and quadrupolar intermolecular forces based on a perturbation theory of Stell et al.[3] and molecular dynamics results of Verlet.[4] These equations were developed assuming point-electrostatic multipoles on nonspherical molecules interacting with a Lennard–Jones intermolecular potential. The suggested quadrupolar expressions were subsequently used in engineering-like equations of state,[5,6] based on the perturbed hard-chain theory (PHCT) EOS.[7] Valderrama and Sandler[8,9] developed a first perturbation theory parameterized for varying molecular elongations based on molecular simulation results for the radial distribution function of fused-sphere molecules. Boublik[10,11] suggested a perturbation theory for elongated molecules by approximating the radial distribution function of a convex molecule by that of the corresponding Gaussian overlap fluid. A renormalized pertur-

Present address of J. Gross: Delft University of Technology, Laboratory for Process Equipment, Leeghwaterstraat 44, 2628 CA Delft, The Netherlands; e-mail: J.Gross@wbmt.tudelft.nl.

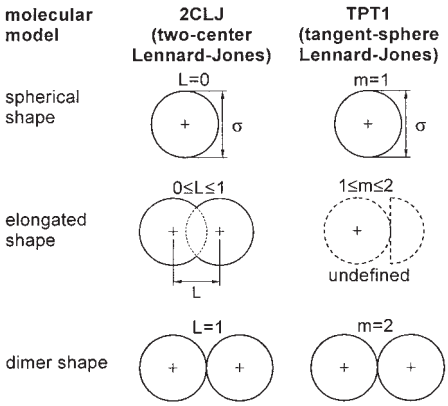

Figure 1. Geometrical setup of the two-center Lennard–Jones (2CLJ) model and the tangent-sphere Lennard–Jones fluid.

bation theory to account for the polarizability of dipolar fluids was already developed in 1977 by Wertheim, by applying a graph-theory approach.[12-14] Gray et al.[15] extended the theory to mixtures and to quadrupolar fluids.

Despite the early progress in modeling polar molecules, however, interactions resulting from permanent charges remain demanding for fluid theories because of the long-range nature of the involved forces. The expansions converge slowly for polar interactions, which is why the *u*-expansion as a common perturbation theory for quadrupolar fluids is of third order and written in the Padé approximation.[3] Nonetheless, when compared to results from molecular simulations the agreement of this approximation is still fairly poor, as indicated by the evaluation of Shing and Gubbins.[16]

An alternative approach was taken by Saager et al.[17] and Saager and Fischer,[18] who extensively performed molecular simulations and obtained a dipole–dipole term and a quadrupole–quadrupole term by fitting empirical expressions to the simulation data. The two-center Lennard–Jones (2CLJ) plus pointdipole fluid and 2CLJ plus pointquadrupole fluid with fixed molecular elongation ($L^* = 0.505$) were considered in their simulations (after studying the effect of molecular elongation[19] on the quadrupolar contribution). The quadrupolar EOS was successfully applied to real substances[20,21] and to mixtures.[22,23] The properties of the 2CLJ plus pointquadrupole fluids were systematically further investigated through molecular simulations for varying molecular elongations by Stoll et al.[24] Although the work of Saager and Fischer has clearly facilitated the fruitful interplay between molecular simulation and EOS development, a restriction of the model is the fixed elongation that, in combination with the empirical nature of the expression, makes it nontrivial to apply to strongly asymmetric mixtures.

The molecular model of tangent spheres is somewhat less elaborate than the 2CLJ model but it has shown to be well suited for strongly asymmetric mixtures. Chapman et al.[25] developed a successful theoretical framework for tangent-sphere molecules and proposed the statistical associating fluid theory (SAFT) EOS based on Wertheim's thermodynamic perturbation theory[26-29] of first order (TPT1). It can be seen from Figure 1 that the tangent-sphere Lennard–Jones (LJ) model is rigorously defined only for integer values of the segment number. When applied to noninteger segment numbers, however, results of the tangent-sphere–LJ model can be brought in accordance with the 2CLJ model.[30]

In this work we will derive an expression for quadrupole–quadrupole interactions. The framework of a third-order perturbation theory (*u*-expansion) is adopted and model constants are adjusted to molecular simulation results of Stoll et al.[24] for the 2CLJ plus quadrupole fluid with varying elongations. The expression is suitable for both the tangent-sphere–LJ model as derived, for example, from the TPT1, and the 2CLJ fluid. In preserving the mathematical framework of a perturbation theory, the model is easily applicable to mixtures of asymmetric systems of "quadrupolar–nonpolar" type. After the model development and the presentation of results for quadrupolar 2CLJ fluids, the model is applied to real substances and mixtures with the perturbed chain (PC)-SAFT EOS.[31,32] A subsequent investigation will be concerned with dipolar fluids and with the inclusion of molecular polarizability.

The Reference-Fluid EOS

The two-center Lennard–Jones plus pointquadrupole fluid consists of two Lennard–Jones sites arranged at a distance L from each other as well as a pointquadrupolar moment Q, positioned between the two sites and aligned along the molecular axis. The intermolecular pair potential can be written as the sum of a 2CLJ fluid and the contribution from the quadrupolar forces

$$u(\mathbf{r}, \omega_i, \omega_j) = u^{2\mathrm{CLJ}}(\mathbf{r}, \omega_i, \omega_j) + u^{QQ}(\mathbf{r}, \omega_i, \omega_j) \tag{1}$$

with $\mathbf{r}$ as the vector pointing from one molecular center to the other and ω_i as a set of two molecular-orientation angles $\{\theta_i, \phi_i\}$. The pair potential of the 2CLJ fluid is conveniently written as a multicenter LJ potential

$$u^{2\mathrm{CLJ}}(\mathbf{r}, \omega_i, \omega_j) = \sum_{\alpha=1}^{2}\sum_{\beta=1}^{2} 4\varepsilon\left[\left(\frac{\sigma}{r_{\alpha\beta}}\right)^{12} - \left(\frac{\sigma}{r_{\alpha\beta}}\right)^{6}\right] \tag{2}$$

where σ and ε are the Lennard–Jones segment size and the segment energy parameter, respectively, and $r_{\alpha\beta}$ is the distance between two sites (LJ centers) of different molecules. The quadrupolar contribution[33] is

$$u^{QQ}(\mathbf{r}, \omega_i, \omega_j) = \frac{3}{4} Q_i Q_j |\mathbf{r}|^{-5} \psi(\omega_i, \omega_j) \tag{3}$$

with ψ as a function of the angles, according to

$$\psi(\omega_i, \omega_j) = 1 - 5c_i^2 - 5c_j^2 - 15c_i^2c_j^2 + 2(s_is_jc - 4c_ic_j)^2 \tag{4}$$

where $s_i = \sin\theta_i$, $c_i = \cos\theta_i$, and $c = \cos(\phi_i - \phi_j)$.

In applying a perturbation theory, the two contributions of the pair potential in Eq. 1 are also treated separately in the EOS; the 2CLJ fluid is considered as the reference fluid, whereas the quadrupolar contribution is regarded as a perturbation. The EOS is written in terms of the residual Helmholtz energy A^{res}, as

Table 1. Pure-Component Parameters of the Tangent-Sphere–LJ Fluid and the 2CLJ Fluid and Conversion Relation between the Two Models

Tangent-Sphere Lennard–Jones		2CLJ (Two-Center Lennard–Jones)	
σ	LJ segment size parameter	σ^{2CLJ}	LJ segment size parameter
ε	LJ segment energy parameter	ε^{2CLJ}	LJ segment energy parameter
m	Number of segments	L	Distance between the two molec. centers
Q^*	Dimensionless quadrupole moment	Q^{*2CLJ}	Dimensionless quadrupole moment

$$\sigma = \sigma^{2CLJ}$$

$$\varepsilon = \frac{4}{m^2}\varepsilon^{2CLJ}$$

$$Q^{*2} = \frac{m}{4}(Q^{*2CLJ})^2$$

$$m = f(L^*) \text{ according to Eq. 7}$$

$$T^* = \frac{m^2}{4}T^{*2CLJ}$$

$$P^* = \frac{m^3}{4}P^{*2CLJ}$$

$$\frac{A^{res}}{NkT} = \frac{A^{2CLJ}}{NkT} + \frac{A^{QQ}}{NkT} \tag{5}$$

where A^{2CLJ} is the Helmholtz energy of the 2CLJ reference fluid, A^{QQ} is the contribution from quadrupole–quadrupole interactions, N denotes the total number of molecules, and k is the Boltzmann constant.

Rather than directly applying a theory for 2CLJ (see, for example, Fischer[34]), we aim at a 2CLJ reference-fluid EOS derived in the TPT1 framework because the TPT1 can also easily be applied to mixtures with strongly nonspherical (chain) molecules. The conformance of both frameworks, however, will be demonstrated below. According to the TPT1, the Helmholtz energy of the reference fluid is obtained as the sum of two contributions, expressed as

$$\frac{A^{2CLJ}}{NkT} = m\frac{A^{LJ}}{NkT} + (1-m)\ln[g^{LJ}(\sigma)] \tag{6}$$

where A^{LJ} is the Helmholtz energy of a Lennard–Jones monomer fluid, m is the number of segments in the chain, and $g^{LJ}(\sigma)$ is the pair correlation function at radial distance σ for a system of spherical Lennard–Jones molecules. The expression of Johnson et al.[35] is used for $g^{LJ}(\sigma)$, whereas the model of Lisal et al.[36] is adopted for the Helmholtz energy of the Lennard–Jones fluid. Both of these equations were derived by fitting empirical expressions to simulation data of the Lennard–Jones fluid and are known to accurately describe LJ properties. It is noteworthy that precise 2CLJ equations of state were proposed by Mecke et al.[37] and Lisal et al.[36] Because we seek to develop a theory for more strongly asymmetric systems, however, we adopt the TPT1 framework (Eq. 6) here.

Although the tangent-sphere–LJ model is not rigorously defined for noninteger segment numbers, it was reported in several studies that the TPT1 can reproduce the properties of a 2CLJ fluid (see Zhou et al.[30] and references therein). Various approaches have been proposed to derive the properties of a two-center model (or, more generally, of a fused-sphere model) from those of a tangent-sphere model, essentially providing different conversion relations between the three pure-component parameters of the 2CLJ fluid and those of the tangent-sphere–LJ fluid. Within our scope it is appealing to find a conversion from the 2CLJ model to the tangent-sphere–LJ fluid where the segment diameter of both models is identical. This scheme for parameter conversion was earlier[30] referred to as approximation A, outlined in Table 1. A high degree of agreement between the reference-fluid EOS (Eq. 6) and molecular simulation data for the 2CLJ fluid is required in this study, and thus no attempt was made to derive a conversion relation between the molecular elongation L^* and the segment number m from theoretical considerations. Rather, the segment number m in Eq. 6 was adjusted to simulation data of the 2CLJ fluid from Stoll et al.[24] and an empirical expression was fitted. The relation thus obtained between elongation L^* and segment number m is displayed in Figure 2 and is given by

$$m = 1 + 0.2177L^* + 3.1498L^{*2} - 3.6738L^{*3} + 1.3063L^{*4} \qquad \text{for } 0 \le L^* \le 1 \tag{7}$$

Using this approximation, the phase-equilibrium properties of a fused-dimer fluid, such as the 2CLJ fluid, can be calculated with good precision considering a tangent-sphere fluid according to the TPT1 framework, and vice versa. Figures 3 and 4 provide a comparison between results from the reference-fluid EOS (Eq. 6) and the simulation data derived by Stoll et al. for various elongations $\{0 \le L^* \le 0.8\}$. Deviations are apparent in the vicinity of the critical point and somewhat in the liquid density region. Given that deviations at the critical point are already observed for a spherical LJ fluid ($L^* = 0$), one may attribute these mismatches partly to an overestimation of the critical point by the LJ EOS in Eq. 6.

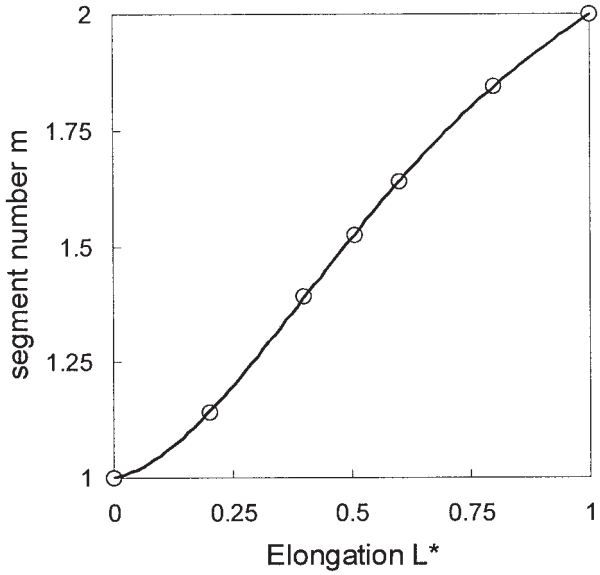

Figure 2. Relation between the molecular elongation *L of the 2CLJ model and the effective segment number *m* of the TPT1 model.**

Symbols are results from adjusting the TPT1 model to simulation data from Stoll et al.[24] and curve is a relation as described in the text.

Theory

It is our goal to derive an expression for quadrupolar interactions from molecular-simulation data, which is valid for varying chain lengths m (or equivalently for varying elongations L^*). Aiming further at a physically based model, which is easy to extend to nonspherical molecules and to mixtures, we start from a perturbation theory (u-expansion) of third order in the Padé approximation, where the Helmholtz energy A^{QQ} is given as

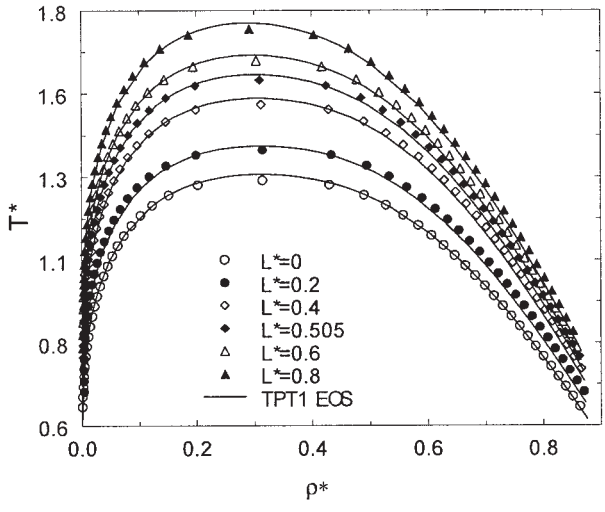

Figure 3. Vapor–liquid equilibrium of the 2CLJ fluid in a temperature–density diagram.

Comparison of the 2CLJ equation of state (EOS) as derived in the TPT1 framework (lines) and simulation data from Stoll et al.[24] (symbols) for six elongations.

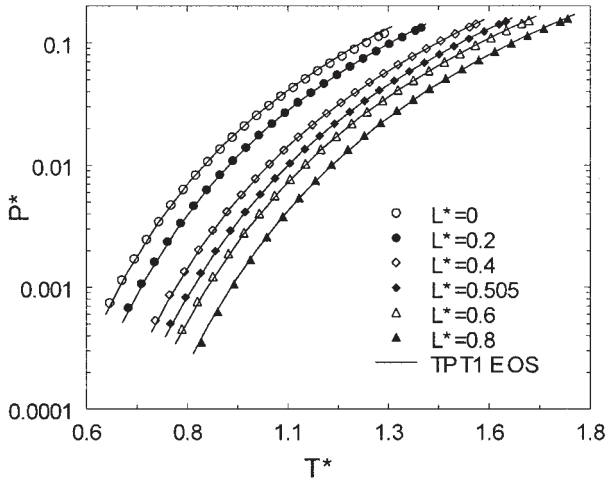

Figure 4. Vapor–liquid equilibrium of the 2CLJ fluid in a pressure–temperature diagram.

Comparison of the 2CLJ EOS as derived in the TPT1 framework (lines) and simulation data from Stoll et al.[24] (symbols) for six elongations.

$$\frac{A^{QQ}}{NkT} = \frac{A_2/NkT}{1 - A_3/A_2} \tag{8}$$

and where A_2 and A_3 are the second-order and third-order perturbation terms, respectively. The first-order term is (as for spherical molecules) cancelled out against an angle-averaged portion of the anisotropic polar pair potential.[10] When linear and symmetric molecules are considered, the second-order and third-order terms for the tangent sphere framework can be written as

$$\frac{A_2}{NkT} = -\pi\left(\frac{3}{4}\right)^2 \rho \sum_i \sum_j x_i x_j \frac{\varepsilon_{ii}}{kT}\frac{\varepsilon_{jj}}{kT}\frac{\sigma_{ii}^5\sigma_{jj}^5}{\sigma_{ij}^7} n_{Q,i} n_{Q,j} Q_i^{*2} Q_j^{*2} J_{2,ij} \tag{9}$$

and

$$\frac{A_3}{NkT} = \frac{\pi}{3}\left(\frac{3}{4}\right)^3 \rho \sum_i \sum_j x_i x_j \left(\frac{\varepsilon_{ii}}{kT}\right)^{3/2}\left(\frac{\varepsilon_{jj}}{kT}\right)^{3/2}\frac{\sigma_{ii}^{15/2}\sigma_{jj}^{15/2}}{\sigma_{ij}^{12}} \times n_{Q,i} n_{Q,j} Q_i^{*3} Q_j^{*3} J_{3,ij} + \frac{4\pi^2}{3}\left(\frac{3}{4}\right)^3 \rho^2 \sum_i \sum_j \sum_k x_i x_j x_k \times \frac{\varepsilon_{ii}}{kT}\frac{\varepsilon_{jj}}{kT}\frac{\varepsilon_{kk}}{kT}\frac{\sigma_{ii}^5\sigma_{jj}^5\sigma_{kk}^5}{\sigma_{ij}^3\sigma_{ik}^3\sigma_{jk}^3} n_{Q,i} n_{Q,j} n_{Q,k} Q_i^{*2} Q_j^{*2} Q_k^{*2} J_{3,ijk} \tag{10}$$

with ρ as the molecular number density, and the dimensionless squared quadrupolar moment $Q_i^{*2} = Q_i^2/(m_i\varepsilon_{ii}\sigma_{ii}^5)$. Similar to the work of Jog and Chapman[38,39] on dipolar molecules, we have introduced $n_{Q,i}$, the number of quadrupolar moments per molecule. For low molecular weight components, such as carbon dioxide, there is only one quadupolar moment of strength Q_i^*, so that $n_{Q,i} = 1$. Values greater than unity are relevant for polar repeat units in a polymer chain or for (bio)molecules with multiple functional groups. Simple Berthelot–Lorentz combin-

ing rules are defined for Eqs. 9 and 10, according to $\varepsilon_{ij} = (\varepsilon_i \varepsilon_j)^{0.5}$ and $\sigma_{ij} = (\sigma_i + \sigma_j)/2$.

The abbreviations $J_{2,ij}$ and $J_{3,ij}$ in Eqs. 9 and 10 are integrals over the reference-fluid pair correlation function and $J_{3,ijk}$ is an integral over three-body correlation functions. To detail the integral $J_{2,ij}$, we have to abandon the TPT1 framework for a moment and rely on the 2CLJ model because the pair correlation function is only then clearly defined and the integral we seek is given[10,11] as

$$J_{2,ij} = m_i m_j \int_0^\infty \bar{r}^{-10} \langle \psi(\omega_i \omega_j)\, g_{ij}^{2\mathrm{CLJ}}(\bar{r}, T, \omega_i \omega_j) \rangle_{\omega_i \omega_j} \bar{r}^2 d\bar{r} \quad (11)$$

where the angle brackets represent shorthand notation for integrations over the orientations and where the dimensionless center-to-center distance $\bar{r} = |\boldsymbol{r}|/\sigma_{ij}$. The integral in Eq. 11 decreases quickly with increasing elongation as Boublik has shown,[10] but much of the dependency of $J_{2,ij}$ on molecular shape is cancelled out through the factor $m_i m_j$.

The angle-dependent pair correlation function $g_{ij}^{2\mathrm{CLJ}}$ of a 2CLJ fluid is not easily available and the integration in Eq. 11 is difficult, however, the resulting dimensionless expression for $J_{2,ij}$ is for a pure fluid only a function of temperature and density and a functional of elongation (or segment number). We adjust expressions for these integrals to molecular simulation data, which enables us to preserve the principal framework of Eqs. 8–10, with the benefit of obvious mixing rules (quadrupolar–nonpolar) and the simple extension to molecules of varying chain lengths. To limit the number of adjustable model constants and in view of the small temperature range covered by the considered simulation data, the $J_{3,ijk}$ integral is assumed to be temperature independent and the $J_{3,ij}$ integral is set to zero. Although the first assumption is valid for molecules with hard repulsion, more generally, it is only a crude approximation. The second assumption can be regarded as the most severe simplification in this work because the treatment of mixtures is somewhat compromised. It may therefore be desirable for a future development to derive the third-order two-body integral ($J_{3,ij}$) directly from correlation results for 2CLJ molecules.

We assume simple power functions for the $J_{2,ij}$ integral and the $J_{3,ijk}$ integral, so that

$$J_{2,ij} = \sum_{n=0}^{4} \left(a_{n,ij} + b_{n,ij} \frac{\varepsilon_{ij}}{kT} \right) \eta^n \quad (12)$$

$$J_{3,ijk} = \sum_{n=0}^{4} c_{n,ijk} \eta^n \quad (13)$$

$$J_{3,ij} = 0 \quad (14)$$

where η is a dimensionless density (also termed packing fraction and defined in the Appendix) and where the coefficients depend on chain length m with

$$a_{n,ij} = a_{0n} + \frac{m_{ij} - 1}{m_{ij}} a_{1n} + \frac{m_{ij} - 1}{m_{ij}} \frac{m_{ij} - 2}{m_{ij}} a_{2n} \quad (15)$$

$$b_{n,ij} = b_{0n} + \frac{m_{ij} - 1}{m_{ij}} b_{1n} + \frac{m_{ij} - 1}{m_{ij}} \frac{m_{ij} - 2}{m_{ij}} b_{2n} \quad (16)$$

and

$$c_{n,ijk} = c_{0n} + \frac{m_{ijk} - 1}{m_{ijk}} c_{1n} + \frac{m_{ijk} - 1}{m_{ijk}} \frac{m_{ijk} - 2}{m_{ijk}} c_{2n} \quad (17)$$

As combining rules for the chain length, we define

$$m_{ij} = (m_i m_j)^{1/2} \quad (18)$$

$$m_{ijk} = (m_i m_j m_k)^{1/3} \quad (19)$$

The expression for covering the chain-length dependency (Eq. 15) was derived by Hu et al.[40,41] in the context of hard-chain molecules, but the arguments leading to Eq. 15 are not limited to repulsive interactions.[31,40] The first constants (a_{0n}, b_{0n}, and c_{0n}) on the righthand side of Eqs. 15–17 determine a spherical fluid ($m = 1$), whereas the second and third terms formally capture the effect of nearest neighbor and next-to-nearest neighbor segments within a chain molecule.

Twu et al.[42] tested different mixing rules of a perturbation theory for polar molecules against molecular simulation data. With the definition of Eqs. 12, 18, and 19 we lean closely to their suggested mixing rule for the case of molecules with spherical reference fluids. For mixtures with only one quadrupolar component, Eq. 18 simplifies to $m_{ii} = m_i$. Whereas the mixture scheme for this case is fairly straightforward, it is more difficult to cope with mixtures with more than one quadrupolar component because the cross-polar interactions for mixtures of real components are often far from those estimated solely from the knowledge of the pure component quadrupolar interactions. It may therefore be advantageous to derive cross-quadrupolar interactions from molecular simulations (on a force-field level or through quantum calculations) rather than from simple mixing rules. The author has not yet elaborated such an approach and the mixing rules Eqs. 18 and 19 have to be considered a first attempt for geometrically similar components.

The model constants of Eqs. 15–17 were adjusted to simulation data for varying chain lengths in a two-step procedure: first, the a_{0n}, b_{0n}, and c_{0n} constants were adjusted to simulation data of spherical molecules and, second, the remaining a_{1n}, a_{2n}, b_{1n}, b_{2n}, and c_{1n}, c_{2n} constants were fitted to simulation data of nonspherical molecules. The adjusted model constants are listed in Table 2.

The proposed quadrupolar equation-of-state contribution can be applied within the 2CLJ framework or with tangent-sphere–based theories, such as the PC-SAFT EOS. More details on the implementation within both frameworks are presented in the Appendix.

Simulation Data

The expression for quadrupole–quadrupole interactions is derived by minimizing the deviation between properties from

Table 2. Model Constants of the Quadrupole Equation-of-State Contribution

i	a_{0i}	a_{1i}	a_{2i}	b_{0i}	b_{1i}	b_{2i}	c_{0i}	c_{1i}	c_{2i}
0	1.2378308	1.2854109	1.7942954	0.4542718	−0.8137340	6.8682675	−0.5000437	2.0002094	3.1358271
1	2.4355031	−11.465615	0.7695103	−4.5016264	10.064030	−5.1732238	6.5318692	−6.7838658	7.2475888
2	1.6330905	22.086893	7.2647923	3.5858868	−10.876631	−17.240207	−16.014780	20.383246	3.0759478
3	−1.6118152	7.4691383	94.486699	0.0	0.0	0.0	14.425970	−10.895984	0.0
4	6.9771185	−17.197772	−77.148458	0.0	0.0	0.0	0.0	0.0	0.0

simulation data for quadrupolar molecules of Stoll et al.[24] and these properties as calculated from our reference-fluid EOS (Eq. 6). The properties considered for the fitting procedure were vapor pressure data, saturated liquid and vapor density data ($0.5T^{*c} \leq T^* \leq 0.99T^{*c}$), critical point data ($T^{*c}$, ρ^{*c}, and P^{*c}), and self-compiled virial coefficients. Elongations L^* of 0, 0.4, 0.505, and 0.8 were considered, corresponding to segment numbers of $m = 1$, 1.3912, 1.5242, and 1.8447, respectively. Values for the quadrupolar moments $(Q^{*,2CLJ})^2$ of 2, 3, and 4 were included (for conversion into Q^* see Table 1). In place of the original simulation data we determined quasi-simulated data from correlations provided by Stoll et al., which allowed generation of a close grid of smoothly aligned data points. The lower temperature limit of $0.5T^{*c}$ is an extrapolation of the simulated data to a subcooled liquid.

It can be seen from Figures 3 and 4 that the reference-fluid EOS does not perfectly agree with results from molecular simulations for the nonpolar case, with $Q^* = 0$. Given that any (systematic) deviation of the reference-fluid EOS from the simulation data leads to incorrect contributions to the determined quadrupole–quadrupole term, we mildly extrapolated the vapor pressure curves. The critical points were not rigorously enforced during the fitting procedure.

Limitations

Model constants of the proposed quadrupole term were obtained by fitting vapor–liquid data and virial coefficients. Additional *PVT* data, enthalpy data, Joule–Thomson inversion points, and so forth were not included in the fitting procedure. Although the lack of simulation data outside the vapor–liquid region is somewhat discomforting, the functional form of the derived expression leans on a perturbation theory providing a sound robustness to extrapolations to supercritical conditions. With respect to the lower temperature condition, the model formally loses its significance at temperatures $< 0.55T^{*c}$ (which is in the solid region for many substances). The power series, however, does not introduce artificial roots in the high-density region down to much lower temperatures.

It was observed that the equation framework did not provide enough flexibility to reproduce the virial coefficients at low temperature and high quadrupole moment with high precision (See Figure 5). This may partially be attributed to neglecting the third-order two-body $J_{3,ij}$ integral but, more important, the third-order u-expansion in general was shown to have deficiencies in the low-density region,[16] which seemingly cannot be compensated for by adjusting the model constants selected herein. Any empirical extension suitable for improving the results for virial coefficients, however, was intentionally avoided to simplify the treatment of mixtures.

Results for the 2CLJ Plus Quadrupole Fluid

Comparisons of the derived EOS with simulation data for the highest available quadrupole moment of $(Q^{*2CLJ})^2 = 4$ and varying molecular elongations are given in Figures 6 and 7. The effect of increasing quadrupolar moments for a fixed molecular elongation $L^* = 0.6$ is illustrated in Figures 8 and 9.

Vrabec et al.[43] adjusted pure-component parameters of the 2CLJ plus pointquadrupole fluid to the properties of 25 real substances, by fitting correlations obtained from their thorough and comprehensive simulation study to experimental data of these components. It is noteworthy that those results can now be reproduced with a consistent thermodynamic model, for which further properties, such as supercritical densities and heat capacities, can also be considered. In a subsequent study, Stoll et al.[24] obtained vapor–liquid data of binary and ternary mixtures from molecular simulation. Figure 10 gives a comparison between simulated data and the proposed theory. The symbols in Figure 10 are predictions of the phase behavior of carbon dioxide and ethane from molecular simulation without correcting the binary interactions. The corresponding line is the analogous prediction from the proposed EOS, where the pure-component parameters are those of the simulation and the binary interaction parameter k_{ij} is also zero. This diagram suggests the mixing rules given above to be suitable for quadrupolar 2CLJ mixtures.

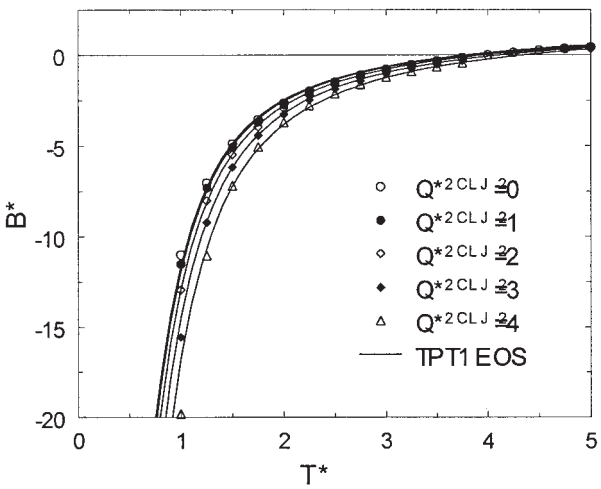

Figure 5. Dimensionless second virial coefficient B^* as a function of temperature.

Comparison of the 2CLJ plus pointquadrupole data with elongation $L^* = 0.8$ and squared quadrupolar moments $(Q^{*2CLJ})^2 = \{0, 1, 2, 3, 4\}$ (symbols) and EOS theory (lines).

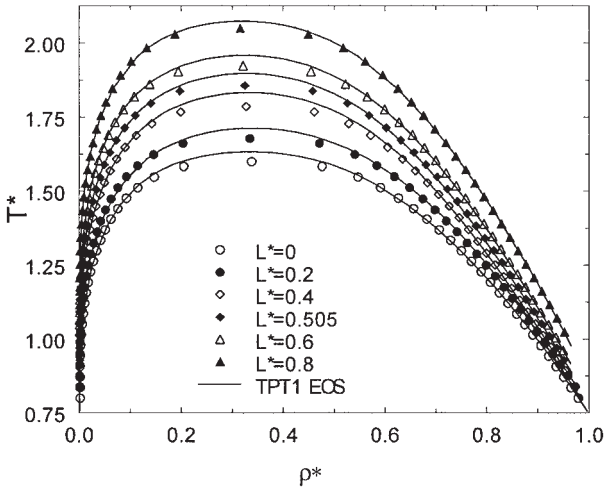

Figure 6. Vapor–liquid equilibrium of the 2CLJ fluid with fixed pointquadrupolar moment of $(Q^{*2CLJ})^2 = 4$ and various molecular elongations.

Comparison of EOS theory (lines) to simulation-data correlations from Stoll et al.[24] (symbols).

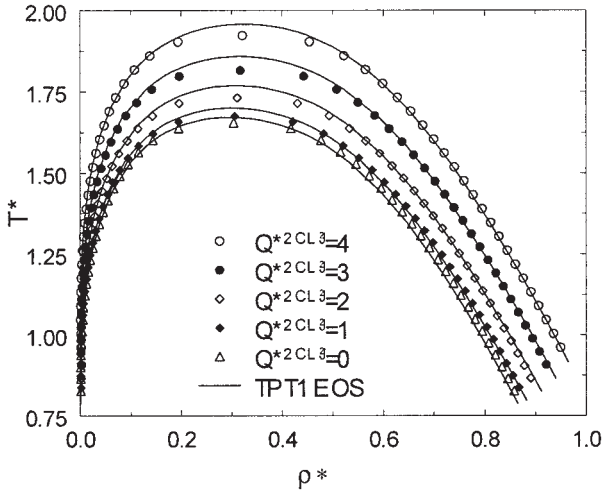

Figure 8. Vapor–liquid equilibrium of the 2CLJ fluid with fixed molecular elongation $L^* = 0.6$ and various squared pointquadrupolar moments $(Q^{*2CLJ})^2$.

Comparison of EOS theory (lines) to simulation-data correlations from Stoll et al.[24] (symbols).

Application to Real Components and Mixtures

The derived quadrupolar expression can readily be incorporated with physically based equations of state for Lennard–Jones chains. It is here applied with the PC-SAFT model. The PC-SAFT EOS is sufficiently compatible with Lennard–Jones chain theories because, during model development, parameters of Lennard–Jones chains were considered for *n*-alkane components. The quadrupolar contribution is considered in the PC-SAFT EOS, by adding Eq. 8 to the appropriate equation of the Helmholtz energy in the PC-SAFT model. Specifics on the implementation are given in the Appendix along with equations for the compressibility factor. For brevity, the EOS is referred to as perturbed-chain polar SAFT (PCP-SAFT).

The molecular quadrupole moment does not have to be treated as an adjustable pure-component parameter in the PCP-SAFT EOS; rather, literature values can be used directly. Quadrupolar, nonassociating compounds are then characterized by three pure-component parameters (segment number m_i, segment diameter σ_i, and segment energy parameter ε_i/k). The pure-component parameters of seven compounds were adjusted to vapor pressure data and liquid density data ranging in temperatures from triple point to critical point. Table A1 presents pure-component parameters along with the absolute average deviation (AAD%) of vapor pressures and of the density data. The obtained deviations in vapor pressure and liquid

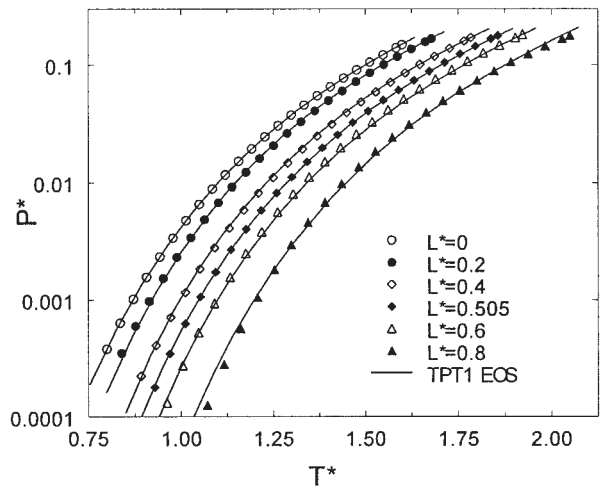

Figure 7. Vapor–pressure curves of the 2CLJ fluid with fixed pointquadrupolar moment of $(Q^{*2CLJ})^2 = 4$ and various molecular elongations.

Comparison of EOS theory (lines) to simulation-data correlations from Stoll et al.[24] (symbols).

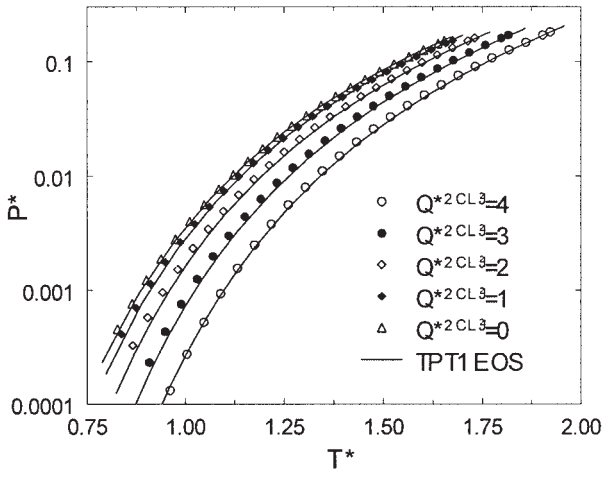

Figure 9. Vapor–pressure curves of the 2CLJ fluid with fixed molecular elongation $L^* = 0.6$ and various squared pointquadrupolar moments $(Q^{*2CLJ})^2$.

Comparison of EOS theory (lines) to simulation-data correlations from Stoll et al.[24] (symbols).

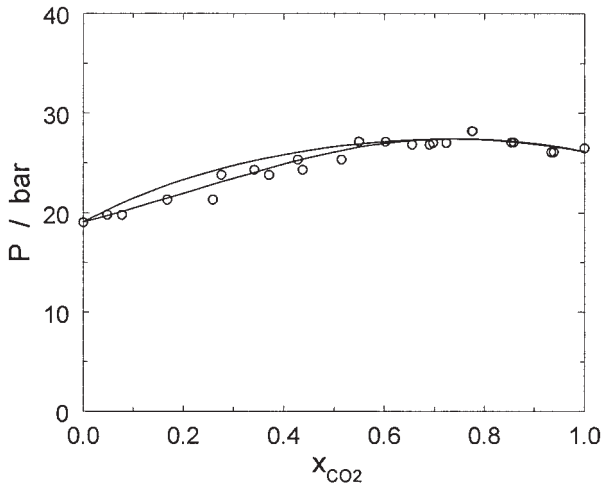

Figure 10. Simulation results[24] for the vapor–liquid equilibrium of a carbon dioxide–ethane mixture at $T = -10$°C considering both components as 2CLJ plus quadrupole fluids and without adjusting the binary interaction between them (symbols).

Model prediction of mixture behavior ($k_{ij} = 0$) using the same pure component parameters as in the simulations (lines).

densities are about equal to or smaller than for the case where the quadrupolar moment was ignored (see values in parentheses in Table A1), although an additional adjustable parameter is not introduced. Particular improvement is observed for strong quadrupolar compounds. Although this result seems expected and nonexiting at first, according to the author's experience with several other perturbation theories considered in the SAFT framework, it is a nontrivial observation. A second set of pure-component parameters is given in Table A1 for each component, where the quadrupolar moment was treated as an adjustable parameter. The resulting values are in good agreement with tabulated values from the literature, thus confirming the physical significance.

The deviations for carbon dioxide as a component with a high volume-specific quadrupolar moment is drastically reduced (using the literature value of $Q = 4.4$ DÅ) to 0.34% in vapor pressure over the complete temperature range from triple point to critical point and 1.27% in liquid, vapor, and supercritical densities. Figure 11 shows the fluid phase behavior of pure carbon dioxide in a pressure vs. density plot. It becomes apparent from Figure 11 that the representation of carbon dioxide's critical region is improved.

Calculation results for mixtures of carbon dioxide with nonpolar compounds are displayed in Figures 12–18. The literature value of $Q = 4.4$ DÅ is considered in all calculations for carbon dioxide. The explicit consideration of quadrupolar interactions improves the overall representation of the phase behavior. A particularly significant improvement is observed at lower temperatures, where carbon dioxide is subcritical or just above its critical temperature. The solubility of carbon dioxide in the carbon dioxide–lean liquid phase is in those cases overestimated, when the quadrupolar interactions are ignored, whereas PCP-SAFT in turn gives systematically improved

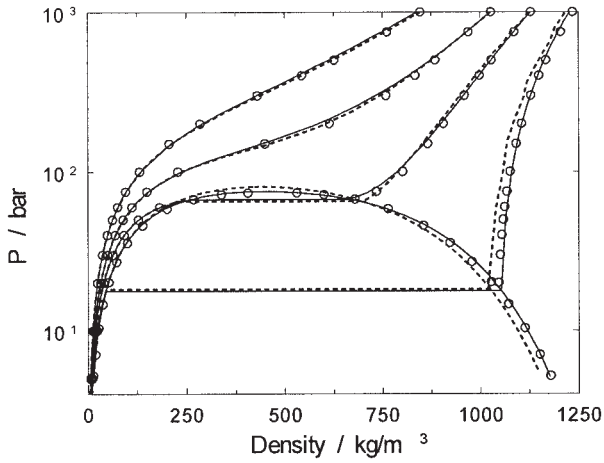

Figure 11. $P\rho T$ behavior of carbon dioxide.

Subcritical and supercritical isotherms and coexisting densities from triple point to critical point from experiment (symbols: IUPAC data; see Table A1), PCP-SAFT EOS (solid lines) and PC-SAFT EOS (short dashed lines).

results. For mixtures at higher temperatures some improvement is observed at mixture-critical points. The adjusted absolute values of the binary interaction parameters are thereby significantly smaller for the proposed model.

The liquid–liquid equilibrium of asymmetric mixtures is a challenging test for fluid theories. An isopleth of the liquid–liquid equilibrium at low temperatures for the system *n*-heptane and carbon dioxide is shown in Figure 14 (along with the mixture critical VL-line). The phase behavior is well described, considering that liquid–liquid data have not been used to regress the k_{ij} parameter. Figure 16 gives another UST (upper solution temperature) liquid–liquid equilibrium for the mixture of *n*-dodecane and carbon dioxide in a temperature–composition diagram. The PCP-SAFT EOS cannot quantitatively reproduce the composition of the carbon dioxide–rich phase. Nevertheless, Figure 16 indicates a substantial improvement over the case where the quadrupolar interactions are ignored,

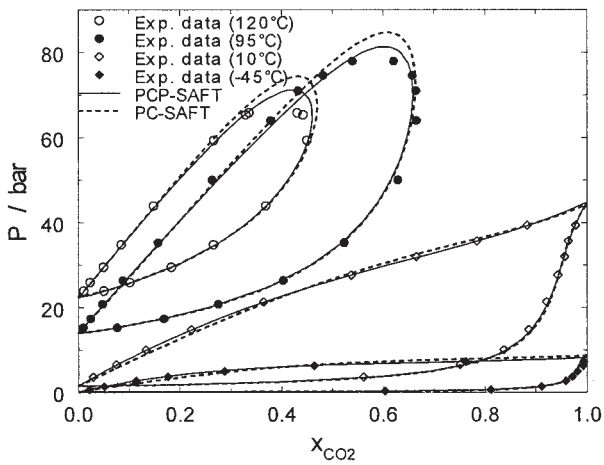

Figure 12. Vapor–liquid equilibrium of *n*-butane–carbon dioxide mixtures at four temperatures.

Comparison of PCP-SAFT ($k_{ij} = 0.036$) and PC-SAFT ($k_{ij} = 0.125$) correlations to experimental data.[47]

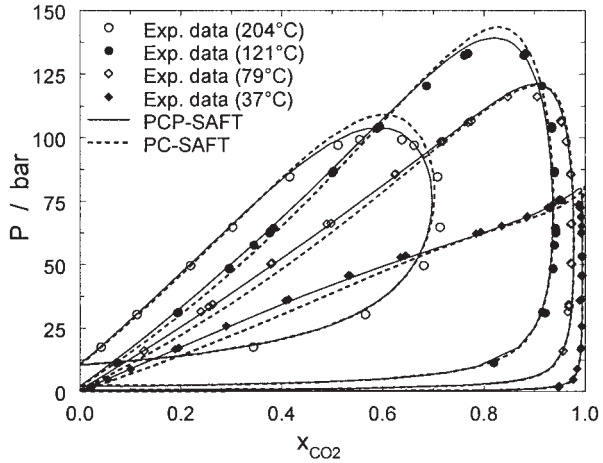

Figure 13. Vapor–liquid equilibrium of *n*-heptane–carbon dioxide mixtures at four temperatures.

Comparison of PCP-SAFT (k_{ij} = 0.039) and PC-SAFT (k_{ij} = 0.110) correlations to experimental data.[48]

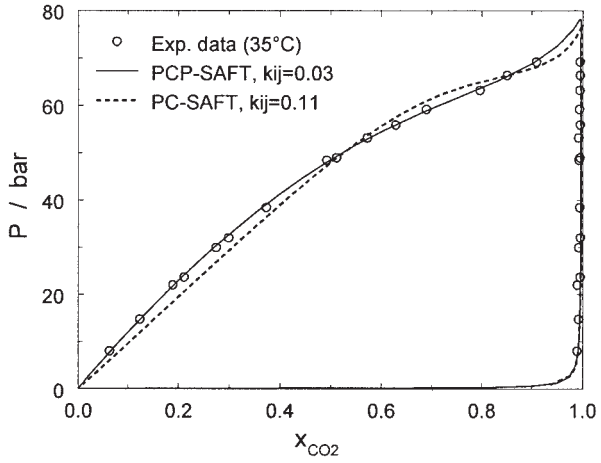

Figure 15. Vapor–liquid equilibrium of a toluene–carbon dioxide mixture at *T* = 35°C.

Comparison of PCP-SAFT (k_{ij} = 0.03) and PC-SAFT (k_{ij} = 0.112) correlations to experimental data.[50]

given that the width of the liquid–liquid area is now considerably better described. A similar behavior can be observed for the mixture of hexadecane and carbon dioxide as well as 1-nonanol and carbon dioxide, as displayed in Figures 17 and 18 in pressure–composition diagrams. The k_{ij} parameters in both cases were adjusted to the mixture-critical pressure. The liquid–liquid equilibrium is substantially wider from the PCP-SAFT EOS and it may also be said that the known tendency of equations of state to overestimate liquid–liquid behavior is reduced.

The nonconformal molecular geometry of real molecules along with the directional nature of polar forces makes the treatment of mixtures with more than one quadrupolar component a difficult task. The charge-distribution and preferential orientation of two benzene molecules, two carbon dioxide molecules, and their crosswise arrangement are illustrated in Figure 19. Benzene and carbon dioxide are oblate and prolate spheroids, respectively, and the cross-quadrupolar interactions for a mixture of both compounds cannot be expected to obey simple mixing rules.

The vapor–liquid equilibrium of benzene and carbon dioxide for three temperatures is shown in Figure 20. The dashed–dotted line gives results for a calculation of two interacting quadrupolar components using the mixing rule proposed above. The calculation result is weaker than for the case where quadrupolar interactions are ignored. The CO_2 solubility in a benzene-rich phase as well as the benzene solubility in a CO_2-rich liquid phase are overestimated. The mixing rule thus overpredicts the crosswise interactions between two quadrupolar compounds. If all crosswise quadrupolar interactions are set to zero ($J_{2,ij} = 0$ for $i \neq j$ and $J_{3,ijk} = 0$ for $i \neq j \neq k$), the

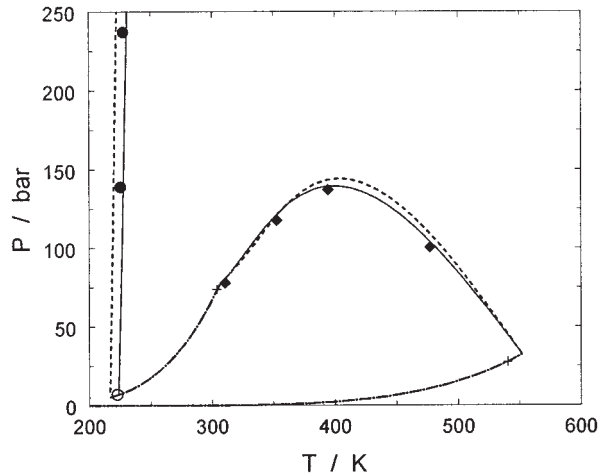

Figure 14. Liquid–liquid isopleth and critical vapor–liquid line of *n*-heptane–carbon dioxide mixtures.

Lines as defined in Figure 13 using same binary interaction parameters. Diamonds: mixture critical points[48]; spheres: liquid–liquid points with 72.5 wt % CO_2[49]; empty sphere: vapor–liquid–liquid point extrapolated from Schneider[49]; and crosses: experimental pure component critical points.

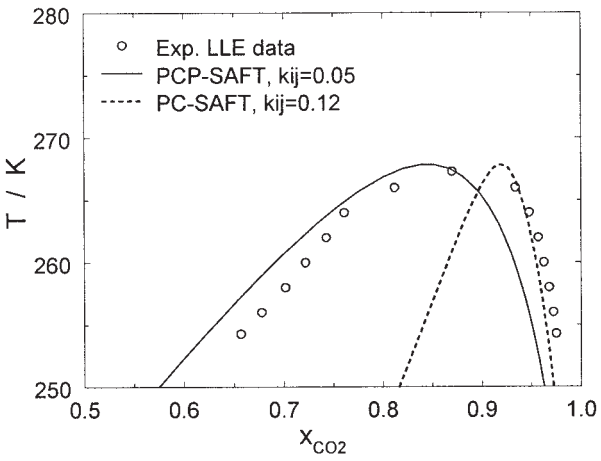

Figure 16. Liquid–liquid–vapor equilibrium of *n*-dodecane–carbon dioxide mixture (UST: upper solution temperature).

Comparison of PCP-SAFT and PC-SAFT correlations to experimental data.[51]

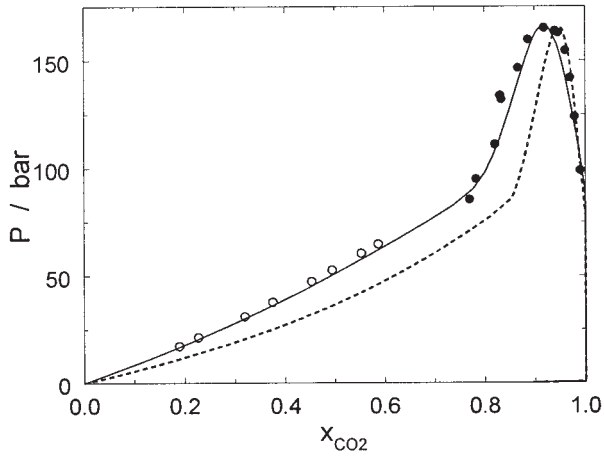

Figure 17. Liquid–liquid and vapor–liquid equilibrium of *n*-hexadecane–carbon dioxide mixture at T = 40°C.

Comparison of PCP-SAFT (k_{ij} = 0.059) and PC-SAFT (k_{ij} = 0.119) correlations to experimental data (VLE[52]; LLE[53]).

description is again better than that for the case where quadrupolar interactions are ignored. This diagram shows that a considerable uncertainty remains related to mixtures with multiple quadrupolar substances and a more systematic investigation of crosswise quadrupolar interactions is desirable.

Conclusions

An equation-of-state (EOS) contribution for quadrupolar components is proposed. The model is based on a third-order perturbation theory written in the Padé approximation. Simple expressions for the dependency on molecular elongations (or chain length) are assumed and model constants were adjusted to comprehensive molecular simulation data of the two-center Lennard–Jones (2CLJ) plus pointquadrupole fluid from the literature.[24] The considered simulation data cover a range of molecular elongations from spherical ($L^* = 0$) to $L^* = 0.8$ and squared reduced quadrupolar moments of $(Q^{*2CLJ})^2 \leq 4$.

It was shown that a reference-fluid EOS derived from the thermodynamic perturbation theory of first order (TPT1) can be used to describe two-center Lennard–Jones (2CLJ) fluids. The proposed model is thus suitable not only for the 2CLJ framework but also for the tangent-sphere Lennard–Jones framework. It was applied to pure components and mixtures of real substances with the PC-SAFT EOS. The representation of pure-component properties is improved, especially for strongly quadrupolar substances. The inclusion of the quadrupole expression leads to systematic improvements for mixtures of a quadrupolar component with nonpolar solvents, as demonstrated for various carbon dioxide mixtures. The required values of the binary interaction parameter were seen to be considerably lower. From these findings, the mixing rule seems appropriate for systems of one quadrupolar component in mix-

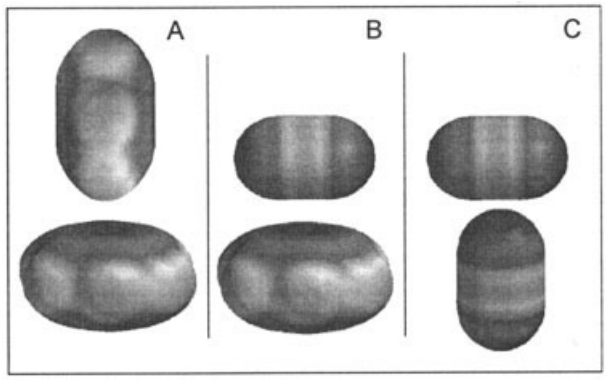

Figure 19. Illustration of surface charge potential of benzene and carbon dioxide and orientational configurations of two molecules.

(A) benzene–benzene; (B) benzene–carbon dioxide; (C) carbon dioxide–carbon dioxide.

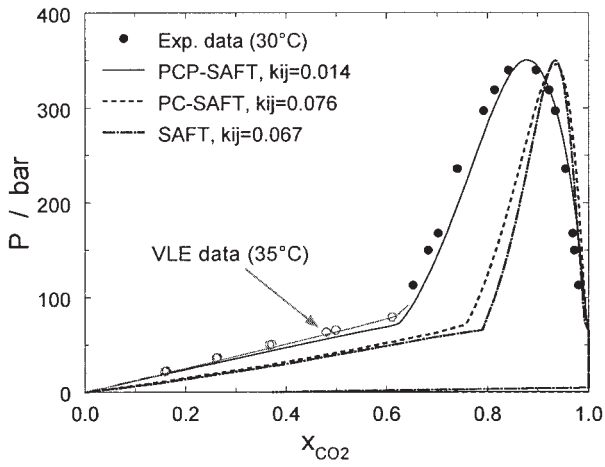

Figure 18. Liquid–liquid equilibrium of a 1-nonanol–carbon dioxide mixture at T = 30°C.

Comparison of PCP-SAFT, PC-SAFT, and SAFT correlations to experimental data.[45] Vapor–liquid equilibrium data[46] and PCP-SAFT correlation using same k_{ij} parameter is displayed also for T = 35°C.

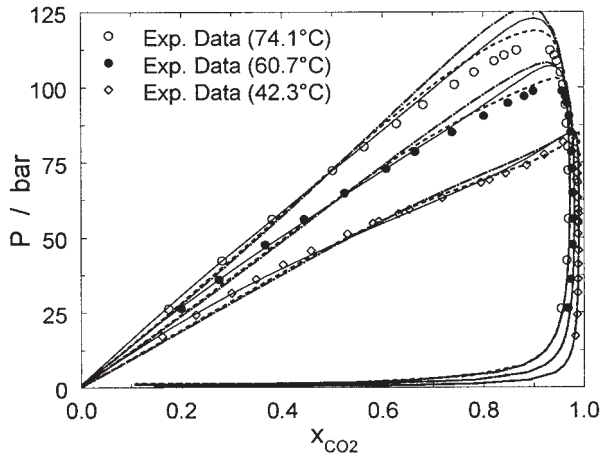

Figure 20. Vapor–liquid equilibrium of benzene–carbon dioxide mixtures at three temperatures.

Symbols are experimental data.[54] Solid line for PCP-SAFT (k_{ij} = 0) with cross-quadrupolar interactions set to zero, dashed–dotted line for PCP-SAFT (k_{ij} = 0.042) with mixing rule for cross-quadrupolar interactions, and short-dashed line for PC-SAFT (k_{ij} = 0.088).

ture with nonpolar components. For mixtures, where both compounds possess a quadrupolar moment, the theory was tested against simulation data and gave a very good result, whereas the mixing rule proved to be unsuitable for real mixtures of more than one quadrupolar component.

Acknowledgments

This study was conducted while the author was employed by BASF AG. The inspiration and constant support of my colleagues at BASF is warmly acknowledged. Further, helpful discussions with Jadran Vrabec are greatly appreciated.

Literature Cited

1. Bungert B, Sadowski G, Arlt W. Separations and material processing in solutions with dense gases. *Ind Eng Chem Res*. 1998;37:3208-3220.
2. Gubbins KE, Twu CH. Thermodynamics of polyatomic fluid mixtures—I. Theory. *Chem Eng Sci*. 1978;33:863-878.
3. Stell G, Rasaiah JC, Narang H. Thermodynamic perturbation theory for simple polar fluids, I. *Mol Phys*. 1972;23:393-406. Some details of the developed theory were published only in subsequent articles: Rushbrooke GS, Stell G, Høye JS. Theory of polar liquids. I. Dipolar hard spheres. *Mol Phys*. 1973;26:1199-1215; Stell G, Rasaiah JC, Narang H. Thermodynamic perturbation theory for simple polar fluids, II. *Mol Phys*. 1974;27:1393-1414.
4. Verlet L. Computer "experiments " on classical fluids. II. Equilibrium correlation functions. *Phys Rev*. 1968;165:201-214.
5. Vimalchand P, Donohue MD. Thermodynamics of quadrupolar molecules: The perturbed-anisotropic-chain theory. *Ind Eng Chem Fundam*. 1985;24:246-257.
6. Cottermann RL, Schwarz BJ, Prausnitz JM. Molecular thermodynamics for fluids at low and high densities. Part I: Pure fluids containing small or large molecules. *AIChE J*. 1986;32:1787-1798.
7. (a) Donohue MD, Prausnitz JM. Perturbed hard chain theory for fluid mixtures. Thermodynamic properties of mixtures in natural gas and petroleum technology. *AIChE J*. 1975;24:849-860; (b) Beret S, Prausnitz JM. Perturbed hard-chain theory—Equation of state for fluids containing small or large molecules. *AIChE J*. 1975;75:1123-1132.
8. Sandler SI. The use of a non-spherical reference potential in statistical mechanical perturbation theory. *Mol Phys*. 1974;28:1207-1223.
9. Valderrama JO, Sandler SI. The use of a non-spherical reference potential in statistical mechanical perturbation theory. III. The Helmholtz free energy and equation of state for pure, quadrupolar fluids. *Mol Phys*. 1983;49:925-936.
10. Boublik T. Perturbation theory for pure quadrupolar hard Gaussian overlap fluids. *Mol Phys*. 1990;69:497-505.
11. Boublik T. Equilibrium behaviour of quadrupolar Kihara molecule fluids. *Mol Phys*. 1991;71:417-426.
12. Wertheim MS. Theory of polar fluids. III. *Mol Phys*. 1977;35:1109-1129.
13. Wertheim MS. Theory of polar fluids. V. Thermodynamics and thermodynamic perturbation theory. *Mol Phys*. 1979;37:83-94.
14. Wertheim MS. Equilibrium statistical mechanics of polar fluids. *Annu Rev Phys Chem*. 1979;30:471-501.
15. Gray CG, Joslin CG, Venkatasubramanian V, Gubbins KE. Induction effects in fluid mixtures of dipolar–quadrupolar polarizable molecules. *Mol Phys*. 1985;54:1129-1148.
16. Shing KS, Gubbins KE. Free energy and vapor–liquid equilibria for a quadrupolar Lennard–Jones fluid. *Mol Phys*. 1982;45:129-139.
17. Saager B, Fischer J, Neumann M. Reaction field simulations of monatomic and diatomic dipolar fluids. *Mol Simulat*. 1991;6:27-49.
18. Saager B, Fischer J. Construction and application of physically based equations of state. Part II. The dipolar and quadrupolar contributions to the Helmholtz energy. *Fluid Phase Equilib*. 1992;72:67-88.
19. Bohn M, Fischer J, Haile JM. Effect of molecular elongation on the quadrupolar free energy in diatomic fluids. *Mol Phys*. 1988;65:797-820.
20. Müller A, Winkelmann J, Fischer J. Backone family of equations of state: 1. Nonpolar and polar pure fluids. *AIChE J*. 1996;42:1116-1126.
21. Calero S, Wendland M, Fischer J. Description of alternative refrigerants with BACKONE equations. *Fluid Phase Equilib*. 1998;152:1-22.
22. Weingerl U, Fischer J. A mixing rule for the quadrupolar contribution to the Helmholtz energy. *Fluid Phase Equilib*. 2000;171:59-76.
23. Weingerl U, Fischer J. Consideration of dipole–quadrupole interactions in molecular based equations of state. *Fluid Phase Equilib*. 2002;202:49-66.
24. Stoll J, Vrabec J, Hasse H, Fischer J. Comprehensive study of the vapour–liquid equilibria of the pure two-centre Lennard–Jones plus pointquadrupole fluid. *Fluid Phase Equilib*. 2001;179:339-362.
25. Chapman WG, Jackson G, Gubbins KE. Phase equilibria of associating fluids. Chain molecules with multiple bonding sites. *Mol Phys*. 1988;65:1057-1079.
26. Wertheim MS. Fluids with highly directional attractive forces: I. Statistical thermodynamics. *J Stat Phys*. 1984;35:19-34.
27. Wertheim MS. Fluids with highly directional attractive forces: II. Thermodynamic perturbation theory and integral equations. *J Stat Phys*. 1984;35:35-47.
28. Wertheim MS. Fluids with highly directional attractive forces: III. Multiple attraction sites. *J Stat Phys*. 1986;42:459-476.
29. Wertheim MS. Fluids with highly directional attractive forces: IV. Equilibrium polymerization. *J Stat Phys*. 1986;42:477-492.
30. Zhou Y, Hall CK, Stell G. Thermodynamic perturbation theory for fused hard-sphere and hard-disk chain fluids. *J Chem Phys*. 1995;103:2688-2695.
31. Gross J, Sadowski G. Application of perturbation theory to a hard-chain reference fluid: An equation of state for square-well chains. *Fluid Phase Equilib*. 2000;168:183-199.
32. Gross J, Sadowski G. Perturbed-chain SAFT: An equation of state based on a perturbation theory for chain molecules. *Ind Eng Chem Res*. 2001;40:1244-1260.
33. Gray CG, Gubbins KE. *Theory of Molecular Fluids*. Vol. I. Oxford, UK: Clarendon Press; 1984.
34. Fischer J. Perturbation theory for the free energy of two-center–Lennard–Jones liquids. *J Chem Phys*. 1980;72:5371-5377.
35. Johnson K, Müller EA, Gubbins KE. Equation of state for Lennard–Jones chains. *J Phys Chem*. 1994;98:6413-6419.
36. Lisal M, Aim K, Mecke M, Fischer J. Revised equation of state for two-center Lennard–Jones fluids. *Int J Thermophys*. 2004;25:159-173.
37. Mecke M, Müller A, Winkelmann J, Fischer J. An equation of state for two-center Lennard–Jones fluids. *Int J Thermophys*. 1997;18:683-698.
38. Jog PK, Chapman WG. Application of Wertheim's thermodynamic perturbation theory to dipolar hard sphere chains. *Mol Phys*. 1999;97:307-319.
39. Jog PK, Chapman WG. Application of dipolar chain theory to the phase behavior of polar fluids and mixtures. *Ind Eng Chem Res*. 2001;40:4641-4648.
40. Hu Y, Liu H, Prausnitz JM. Equation of state for fluids containing chainlike molecules. *J Chem Phys*. 1996;104:396-404.
41. Liu H, Hu Y. Molecular thermodynamic theory for polymer systems II. Equation of state for chain fluids. *Fluid Phase Equilib*. 1996;122:75-97.
42. Twu CH, Gubbins KE, Gray CG. Thermodynamics of mixtures of nonspherical molecules. III. Fluid phase equilibria and critical loci. *J Chem Phys*. 1976;64:5186-5197.
43. Vrabec J, Stoll J, Hasse H. A set of molecular models for symmetric quadrupolar fluids. *J Phys Chem B*. 2001;105:12126-12133.
44. Stoll J, Vrabec J, Hasse H. Vapor–liquid equilibria of mixtures containing nitrogen, oxygen, carbon dioxide, and ethane. *AIChE J*. 2003;49:2187-2198.
45. Pfohl O, Pagel A, Brunner G. Phase equilibria in systems containing *o*-cresol, *p*-cresol, carbon dioxide, and ethanol at 323.15–473.15 K and 10–35 MPa. *Fluid Phase Equilib*. 1999;157:53-79.
46. Chang CJ, Chiu K-L, Day C-Y. A new apparatus for the determination of P–x–y diagrams and Henry's constants in high pressure alcohols with critical carbon dioxide. *J Supercrit Fluids*. 1998;12:223-237.
47. Kalra H, Krishnana TR, Robinson DB. Equilibrium-phase properties of carbon dioxide–butane and nitrogen–hydrogen sulfide systems at subambient temperatures. *J Chem Eng Data*. 1976;21:222-225.
48. Kalra, H, Kubota H, Robinson DB, Ng H-J. Equilibrium phase properties of the carbon dioxide–*n*-heptane system. *J Chem Eng Data*. 1978;23:317-321.
49. Schneider G. Pressure effect on the phase separation of liquid systems. IV. Phase separation in liquid *n*-alkane–CO_2 systems up to $-60°$ and 1500 bars. Measurements related to the problem of "phase separation in gases. " *Ber Bunsen-Ges* 1966;70:10-16.

50. Fink SD, Hershey HC. Modeling the vapor–liquid equilibria of 1,1,1-trichloroethane + carbon dioxide and toluene + carbon dioxide at 308, 323, and 353 K. *Ind Eng Chem Res*. 1990;29:295-306.
51. Hottovy JD, Luks KD, Kohn JP. Three-phase liquid–liquid–vapor equilibriums behavior of certain binary carbon dioxide–*n*-paraffin systems. *J Chem Eng Data*. 1981;26:256-258.
52. Tanaka H, Yamaki Y, Kato M. Solubility of carbon dioxide in pentadecane, hexadecane, and pentadecane + hexadecane. *J Chem Eng Data*. 1993;38:386-388.
53. Nieuwoudt I, du Rand M. Measurement of phase equilibria of supercritical carbon dioxide and paraffins. *J Supercrit Fluids*. 2002;22:185-199.
54. Bendale PG, Enick RM. Use of carbon dioxide to shift benzene/acetonitrile and benzene/cyclohexane azeotropes. *Fluid Phase Equil*. 1994;94:227-253.

Appendix

This appendix provides details on the implementation of the proposed quadrupole equation-of-state (EOS) contribution within the 2CLJ-fluid framework as well as with the PC-SAFT EOS and presents expressions for calculating the compressibility factor.

Implementation with Eq. 6

For pure 2CLJ plus pointquadrupole fluids, the second- and third-order terms of the quadrupolar contribution simplify to

$$\frac{A_2}{NkT} = -\frac{9\pi}{16}\rho^* \frac{1}{T^{*2}} Q^{*4} J_{2,ij} \tag{A1}$$

$$\frac{A_3}{NkT} = \frac{9\pi^2}{16}\rho^{*2} \frac{1}{T^{*3}} Q^{*6} J_{3,ijk} \tag{A2}$$

where ρ^* ($=\rho/\sigma^3$) is the dimensionless molecular density of the 2CLJ fluid. To evaluate the two expressions for the LJ fluid in Eq. 6 a dimensionless segment density needs to be introduced, according to $\rho_s^* = \rho^* m$, where the segment number m is determined using Eq. 7. The segment density according to the LJ model[36] of Eq. 6 is in turn related to the packing fraction, by[36]

$$\eta = \rho_s^* 0.5256\left[0.67793 + (1 - 0.67793) \times \left(\frac{T^*}{0.25\sqrt{34.037352}}\right)^{0.3674}\right]^{-1} \tag{A3}$$

Implementation with the PC-SAFT EOS

The compressibility factor contribution of the proposed quadrupole–quadrupole term is a residual property that simply adds to the overall compressibility of an EOS. In the case of the PC-SAFT EOS it is added to the hard-chain contribution Z^{hc}, the dispersion term Z^{disp}, and the association term Z^{assoc} as

$$Z = 1 + Z^{hc} + Z^{disp} + Z^{assoc} + Z^{QQ} \tag{A4}$$

The compressibility-factor contribution is then calculated from the thermodynamic relation for residual properties as

$$Z^{QQ} = \eta\left[\frac{\partial(F^{QQ}/NkT)}{\partial\eta}\right]_{T,x_i} = \frac{\tilde{a}_2(\tilde{a}_2\tilde{a}_{2\eta} - 2\tilde{a}_3\tilde{a}_{2\eta} + \tilde{a}_2\tilde{a}_{3\eta})}{(\tilde{a}_2 - \tilde{a}_3)^2} \tag{A5}$$

where, for brevity, we have introduced abbreviations for the reduced Helmholtz energy as

Table A1. PCP-SAFT Pure-Component Parameters for Quadrupolar Components

Substance	M (g/mol)	m	σ (Å)	ε/k (K)	$\lvert Q\rvert$ (DÅ)*	AAD% PC-SAFT) P^{sat}	AAD% PC-SAFT) ρ	Data Ref.**
Carbon dioxide	44.01	1.5131	3.1869	163.33	4.4†	0.34 (2.78)	1.27‡ (2.73‡)	1
		1.6298	3.0867	163.34	3.9546	0.20 (2.78)	1.27‡ (2.73‡)	
Carbon disulfide	76.143	1.5876	3.7106	342.08	4.26†	2.30 (2.28)	0.90 (0.77)	2
		1.3906	3.9453	344.25	7.3662	0.73 (2.28)	0.99 (0.77)	
Ethylene	28.05	1.5425	3.4523	179.37	2.0†	0.57 (1.16)	1.18‡ (2.61‡)	3, 4
		1.5477	3.4475	179.19	1.9155	0.57 (1.16)	1.18‡ (2.61‡)	
Acetylene	26.04	1.5477	3.3428	174.48	4.6†	0.31 (0.42)	0.58 (0.88)	5, 6, 7
		1.5587	3.3325	174.68	4.5415	0.31 (0.42)	0.56 (0.88)	
Nitrogen	28.01	1.1504	3.3848	91.40	1.43†	0.48 (0.34)	1.51 (1.50)	8
		1.1879	3.3353	90.99	1.1151	0.30 (0.34)	1.54 (1.50)	
Chlorine	70.905	1.3934	3.5339	270.49	4.1†	1.34 (0.99)	0.55 (0.57)	2
		1.4682	3.4480	269.67	3.0724	0.98 (0.99)	0.50 (0.57)	
Benzene	78.114	2.2463	3.7852	296.24	5.5907	0.29 (0.64)	1.08 (1.42)	2, 5

Note: Two sets of parameters are given for each component, one using the literature value of the quadrupolar moment Q and one parameter set with Q adjusted to pure-component data.

*DÅ = 3.3356×10^{40} cm^2 ($=10^{-26}$ erg$^{1/2}$ cm$^{5/2}$).

**References: (1) International Union of Pure and Applied Chemistry. *International Thermodynamic Tables of Fluid State: Carbon Dioxide.* Oxford, UK: Pergamon Press; 1973; (2) Daubert TE, Danner RP, Sibul HM, Stebbins CC. *Physical and Thermodynamic Properties of Pure Chemicals: Data Compilation.* Washington, DC: Taylor & Francis; 1989; (3) Nowak, P, Kleinrahm R, Wagner W. *J Chem Thermodyn.* 1196;28:1423–1439; (4) Nowak P, Kleinrahm R, Wagner W. *J Chem Thermodyn.* 1996;28:1441–1460; (5) *VDI-Wärmeatlas.* Düsseldorf, Germany: VDI-GVC; 1994; (6) Korea Thermophysical Properties Data Bank. http://www.cheric.org/kdb/; (7) Landolt-Börnstein. *Gleichgewichte ausser Schmelzgleichwichten.* Band II, Teil 2. Berlin: Springer-Verlag; 1960; (8) International Union of Pure and Applied Chemistry. *International Thermodynamic Tables of Fluid State: Nitrogen.* Oxford, UK: Pergamon Press; 1979.

†First parameter set of each component uses the literature value for Q. Considered are average values from induced birefringence (IB) measurements compiled from Gray CG, Gubbins KE. *Theory of Molecular Fluids.* Vol. 1. Oxford, UK: Clarendon; 1984. No IB values therein are available for acetylene and values from "pressure second virial coefficient" adjustments were used. Benzene is assumed to possess only one axis of charge.

‡Supercritical density data were also used.

$$\tilde{a}_2 = \frac{A_2}{NkT} \tag{A6}$$

and for the appropriate derivatives to density

$$\tilde{a}_{2\eta} = \left[\frac{\partial(A_2/NkT)}{\partial\eta}\right]_{T,x_i} \tag{A7}$$

The packing fraction is for the PC-SAFT EOS, defined by

$$\eta = \frac{\pi}{6}\rho \sum_k x_i m_i d_i^3 \tag{A8}$$

where the temperature-dependent effective segment diameter of component i is expressed as

$$d_i = \sigma_{ii}\left[1 - 0.12\exp\left(-3\frac{\varepsilon_{ii}}{kT}\right)\right] \tag{A9}$$

The density derivatives for the second- and third-order terms in Eq. A5 are given by

$$\tilde{a}_{2\eta} = -\frac{9\pi}{16}\frac{\rho}{\eta}\sum_i\sum_j x_i x_j \frac{\varepsilon_{ii}}{kT}\frac{\varepsilon_{jj}}{kT}\frac{\sigma_{ii}^5\sigma_{jj}^5}{\sigma_{ij}^7} n_{Q,i}n_{Q,j}Q_i^{*2}Q_j^{*2}(\eta J_{2,ij})_\eta \tag{A10}$$

$$\tilde{a}_{3\eta} = \frac{9\pi^2}{16}\left(\frac{\rho}{\eta}\right)^2 \sum_i\sum_j\sum_k x_i x_j x_k \times \frac{\varepsilon_{ii}}{kT}\frac{\varepsilon_{jj}}{kT}\frac{\varepsilon_{kk}}{kT}\frac{\sigma_{ii}^5\sigma_{jj}^5\sigma_{kk}^5}{\sigma_{ij}^3\sigma_{ik}^3\sigma_{jk}^3} n_{Q,i}n_{Q,j}n_{Q,k}Q_i^{*2}Q_j^{*2}Q_k^{*2}(\eta^2 J_{3,ijk})_\eta \tag{A11}$$

where

$$(\eta J_{2,ij})_\eta = \sum_{n=0}^{4}\left(a_{n,ij} + b_{n,ij}\frac{\varepsilon_{ij}}{kT}\right)(n+1)\eta^n \tag{A12}$$

$$(\eta^2 J_{3,ijk})_\eta = \sum_{n=0}^{4} a_{n,ijk}(n+2)\eta^{n+1} \tag{A13}$$

The notation in this work is compatible with that proposed by Gross and Sadowski[32] and ρ is defined as the molecular number density in units [$Å^{-3}$]. The fraction (ρ/η) in Eqs. A10 and A11 is according to Eq. A8 a function of temperature and composition.

Finally, let us consider the quadrupole moment, which is most commonly tabulated in units [DÅ] or with equal values in units [10^{-26} $erg^{1/2}$ $cm^{5/2}$] (for conversion into SI units refer to Table A1). The dimensionless quadrupole moment of component i is defined as

$$Q_i^{*2} = \frac{Q_i^2 \times 10^{-69}\,\frac{Jm^5}{(DÅ)^2}}{m_i(\varepsilon_{ii}/k)k\sigma_{ii}^5 \times 10^{-50}\,\frac{m^5}{Å^5}} \tag{A14}$$

where the Boltzmann constant is $k = 1.380658$ J/K and where the pure component parameter ε_{ii}/k is given in unit [K] and σ_{ii} in unit [Å].

Manuscript received Aug, 25, 2004, and revision received Jan. 6, 2005.